Article

The Influence of a Commercial Few-Layer Graphene on the Photodegradation Resistance of a Waste Polyolefins Stream and Prime Polyolefin Blends

S. M. Nourin Sultana [1], Emna Helal [1,2], Giovanna Gutiérrez [2], Eric David [1,*], Nima Moghimian [2] and Nicole R. Demarquette [1,*]

1 Mechanical Engineering Department, Ecole de Technologie Superieure, 1100 Notre-Dame Street West, Montréal, QC H3C 1K3, Canada; emna.helal@etsmtl.ca (E.H.)

2 NanoXplore Inc., 4500 Thimens Blvd, Montréal, QC H4R 2P2, Canada; giovanna.gutierrez@nanoxplore.ca (G.G.)

* Correspondence: eric.david@etsmtl.ca (E.D.); nicoler.demarquette@etsmtl.ca (N.R.D.)

Abstract: This work investigated the photostabilizing role of a commercially available few-layer graphene (FLG) in mixed polyolefins waste stream (MPWS), ensuring extended lifespan for outdoor applications. The investigation was conducted by analyzing carbonyl content increase, surface appearance, and the retention of mechanical properties of UV-exposed MPWS/FLG composites. Despite the likely predegraded condition of MPWS, approximately 60%, 70%, 80%, and 90% of the original ductility was retained in composites containing 1, 4, 7, and 10 wt.% FLG, respectively. Conversely, just 20% of the original ductility was retained in unfilled MPWS. Additionally, less crack density and lower carbonyl concentrations of the composites also highlighted the photoprotection effect of FLG. For prime polyolefin blends, only 0.5 wt.% or 1 wt.% FLG was sufficient to preserve the original surface finishing and protect the mechanical properties from photodegradation. Hence, it was observed that MPWS requires more FLG than prime polyolefin blends to get to comparable property retention. This could be attributed to the poor dispersion of FLG in MPWS and inevitable uncertainties such as the presence of impurities, pre-degradation, and polydispersity associated with MPWS. This study outlines a potential approach to revalorize MPWS that possess a minimal intrinsic value and would otherwise be destined for landfill disposal.

Keywords: graphene; polyolefin; waste; photodegradation; photoprotection; mechanical properties

1. Introduction

Worldwide, approximately 350 million metric tons (Mt) of plastic waste are generated each year, and a substantial part, approximately 50%, is composed of polyolefin mixture [1]. Therefore, the development of effective strategies to revalorize mixed polyolefins waste stream (MPWS) would pave the way to utilize a significant portion [2] of plastic waste with a small or no base commercial value that would otherwise be disposed off in landfills. Consequently, the scientific research on reusing post-consumer waste-recovered polyolefin blends is getting more attention. Several studies have been developed targeting the modification of mechanical properties of MPWS [3–7] through, for instance, the addition of copolymers or rigid fillers. However, the photodegradation [8–11] of polyolefins is a key challenge that should be successfully resolved to attain an extended lifespan in outdoor applications, such as containers, bumpers, dashboards, garden furniture, playground equipment, bottle crates, etc.

Photodegradation is initiated when internal or external light-absorbing groups (chromophore groups) of a polymer absorb photons from the UV radiation (wavelength ≤400 nm) of sunlight. This irreversible phenomenon may alter the chain length, mechanical properties, and appearance (color and surface finish) [12] of materials. In turn, the performance of

the materials is compromised. The photodegradation of polymeric materials is governed by two influential steps [13,14]:

Initiation: The production of primary radicals due to the absorption of photons by chromophore groups.

Propagation: The production of successive polymer radicals due to the attack of primary radicals on the polymer chains, followed by consequential crosslinking or chain scission.

These things considered, photodegradation of polymers is mainly governed by the presence of chromophore groups [15]. Chromophores can be both internal and external (catalyst, solvents, additives, in-chain or end-chain unsaturated double bonds, etc.). For example, the photodegradation of polyolefins is caused by the presence of external impurities [13,14], which might have been produced during polymerization and post-polymerization processing steps. Additionally, chromophores can be an integrated group into the polymer chains. For instance, photodegradation of poly(styrene) (PS) is mainly caused by the presence of UV-absorbing aromatic groups [16]. Traditionally, rigid filler (carbon black [15]) or different chemicals (phenolic/nonphenolic UV absorbers [17], hindered amines [18], and phenolic antioxidants) are used as photostabilizing additives to protect thermoplastics from photodegradation. However, some of these additives are associated with health concerns [19,20], toxicity [21], and the migration of small molecules over time.

Concomitantly, graphene, a carbon-based material, is gaining attention as a prospective photostabilizer due to the presence of π bonds and two-dimensional (2D) geometry [8]. The chemical structure enables graphene to absorb light in the UV region, through π → π*transitions [22,23], while the 2D structure allows it to act as a physical barrier to small molecules [24–26]. Additionally, a recent study has confirmed that few-layer (6 to 10 layers) graphene (FLG) does not have the same adverse dermal, inhalation, and gene toxicity effects that are well-known for other nanocarbons [27]. Therefore, FLG is expected to be a safer option over some traditionally used photostabilizers. Consequently, different graphene derivatives (graphene, graphene oxide GO, and reduced graphene oxide) have been investigated to photostabilize several polymers [28–33].

In the case of polymer blends, the photostability depends on the blend composition and chemical structure of individual phases, as well as the interaction between the respective blend components. Several studies on the photostability of blends have been summarized by Manita et al. [34]. Some results, as reported in the literature, are listed in Table 1, along with key findings of the present work.

Table 1. Photooxidation behavior of several polymer blends compared to that of their component polymers, cited in the literature.

Polymer Blend System	Findings of the Authors on Photostability	Ref.
Polycaprolactone(PCL)/Poly (vinyl chloride) (PVC)	A positive interaction effect of the components resulted in an increased photostability of the blend compared to that of the homopolymers.	[35]
PP/high impact polystyrene (HIPS)	The blend was found to be more photostable than pure PP as a result of the opacity of the blend and the larger scattering effect by the phase interface.	[36]
PS/poly(viny1 acetate) (PVAc)	An accelerated photodegradation tendency of the blend was reported. The degradation behavior was found to be significantly influenced by the composition and morphology of the blend.	[37]
Poly(vinyl methyl ether) (PVME)/PS	The photodegradation of the blend was deemed to be governed by the photooxidation trend of PVME.	[38]
PP/poly(butylene terephthalate) (PBT)	The photodegradation of the blend was considered to involve both photolytic degradation and photooxidation of PBT sequence.	[39]

Table 1. *Cont.*

Polymer Blend System	Findings of the Authors on Photostability	Ref.
Low-density polyethylene (LDPE)/cellulose	The blend was reported to be less photostable and more biodegradable than the pure components.	[40]
Liner low-density polyethylene (LLDPE)/plastic waste (46 wt.% LLDPE, 51 wt.% LDPE, 1 wt.% HDPE, and 2 wt.% PP)	The presence of plastic waste was found to affect the photostability of pure LLDPE.	[41]
LLDPE/LDPE	The addition of carbonaceous fillers (carbon black, carbon nanotube and graphene) was found to improve the photostability of the blend composite.	[42]
(1) MPWS (2) prime PE/PP	The addition of commercial-grade few-layer graphene resulted in the retardation of photodegradation of the blend systems.	**This work**

A range of comprehensive studies on the photodegradation process of different polymer blends is available in the literature [1–8]. Photoprotection of polymer blends, however, has rarely been addressed. In particular, no study has been found to report the photostabilizing influence of commercial-grade few-layer graphene in PE/PP blend systems. Therefore, this work aims to explore the photostabilizing potential of a commercial few-layer graphene to extend the lifetime of polyolefin blends, for both a mixed waste stream, as well as a prime PE/PP control blend. It is worth mentioning that the used graphene is produced by an environment-friendly mechanochemical exfoliation process. The collaborating research group of this study has previously reported that the addition of such commercial-grade FLG can improve mechanical properties of a polyolefins waste stream [3,43]. The potential of this FLG to enhance UV protection would eliminate or significantly reduce the use of traditional photostabilizers, and also increase the lifetime of post-consumer waste-recovered polymer, intending for outdoor application.

2. Results and Discussion

2.1. Morphology

Figure 1 shows the morphology of the waste polyolefins mixture and neat prime PE/PP—60/40 blend. Here, the rough phase corresponds to PE phase and the smoother phase represents the PP phase of the blend, as indicated in Figure 1. The morphology of control polyolefin blend mimics the microstructure of MPWS.
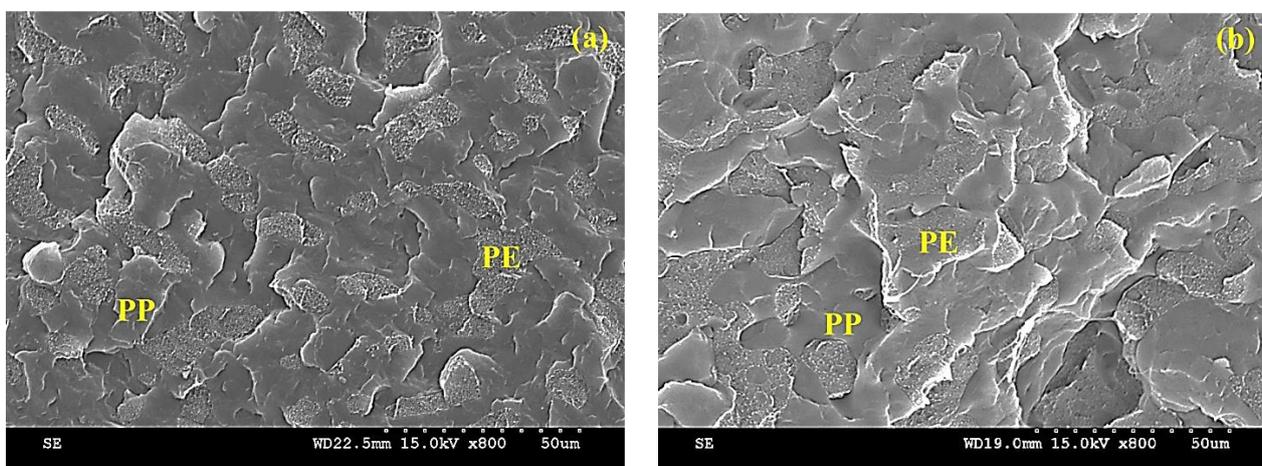

Figure 1. SEM image of (**a**) MPWS and (**b**) neat prime PE/PP—60/40 blend.

Figure 2a–c2 illustrate the microstructure of the compression molded MPWS composite and prime PE/PP—60/40 blend composite, containing 1 wt.% FLG. Figure 2a shows that preferentially, FLG localizes to PE phase, which was also reported in our previous work [3] for the composite containing 4 wt.% FLG. Similarly, Figure 2b, representing the composite where FLG was premixed with PE, shows that FLG is selectively localized in PE phase without any indication of FLG migration to PP phase. In contrast, Figure 2c1,c2, representing the composite where FLG was premixed with PP, indicate that FLG is located in both PP phase and PE/PP interface. This localization of FLG in PE/PP interface is an indication of the preference of FLG towards PE over PP. A similar observation was reported in the literature [44].
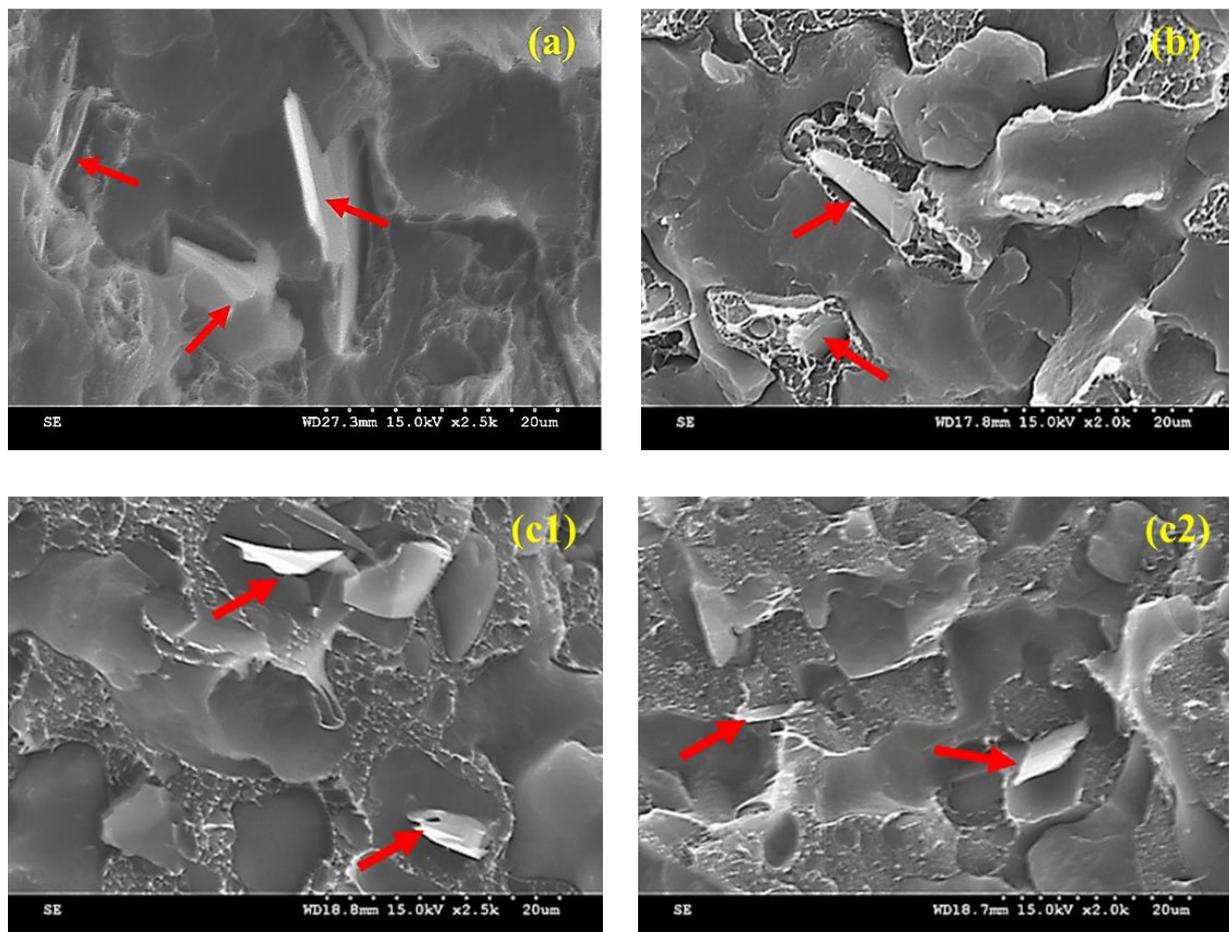

Figure 2. SEM images of 1 wt.%-FLG-filled (**a**) MPWS composite, prime PE/PP blend composite; (**b**) FLG premixed with PE phase, (**c1,c2**) FLG premixed with PP phase and the localization of FLG has been marked by the red arrow to guide the readers' eyes.

2.2. Dispersion of FLG

Figure 3a,b display the processed optical microscope images of thin film of MPWS and prime PE/PP composites, respectively, each containing 1 wt.% of FLG. Dark regions represent FLG particles and the white background represents the polymeric phases of the composites. Additionally, Figure 3c illustrates the frequency of FLG agglomerates as a function of agglomerate area in the composites to quantify the dispersion of FLG in MPWS and prime PE/PP blend. The grey bars represent the agglomerate size distribution in the prime blend composite, while the black bars represent the distribution in MPWS composite.
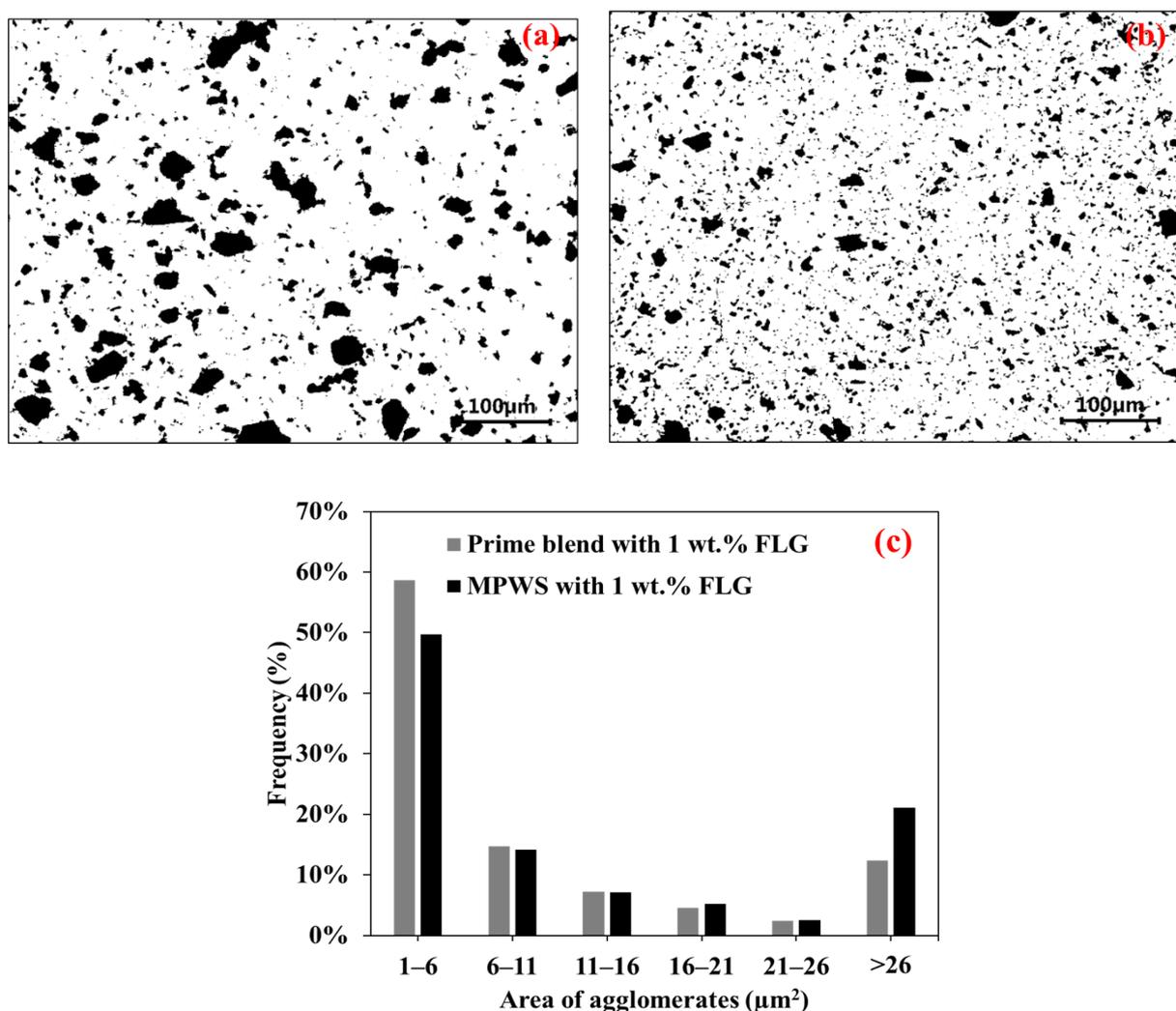
Figure 3. The representation of FLG dispersion in (**a**) MPWS and (**b**) prime polyolefin blend along with (**c**) the frequency of FLG agglomerates in 1 wt.% FLG-filled MPWS and prime PE/PP blend as a function of FLG agglomerate area.

Remarkably larger agglomerates can be seen in Figure 3a, indicating poor dispersion of FLG in the MPWS composite. Conversely, the prime PE/PP composite exhibits better dispersion with smaller FLG agglomerates. This difference in dispersion of FLG could be attributed to dissimilar rheological property of the polymer content of the composites. Notable differences can be observed at the two extremes of the X-axis, representing the size ranges of the agglomerates. It is observed that prime blend composite possesses higher percentage (~60%) of smaller FLG agglomerates than that (~50%) of MPWS composite or vice versa. Despite following similar processing conditions, different FLG dispersion is observed in two different matrices. To investigate the root cause, the MFI value of MPWS and prime PE/PP blend was measured. The MFI of MPWS and prime blend was found to be 12 ± 2 g/10 min and 3 ± 0.5 g/10 min, respectively. Hence, prime PE/PP blend of this work is much more viscous than MPWS. During melt mixing, higher viscosity-driven shear stress would have facilitated better dispersion of FLG in viscous prime PE/PP blend than in comparatively less viscous MPWS of this work. It is worth mentioning that better dispersion in more viscous matrices was also observed by other authors [45].

2.3. Effect of Adding FLG on UV-Exposed Composites

2.3.1. Chemical Analysis

In Figure 4, calculated carbonyl index of prime PE/PP blend and MPWS have been plotted along with error bars (standard deviation for the replicas of each sample) as a function of exposure time. The carbonyl index (CI) was calculated by analyzing the FTIR absorption spectra of the respective polyolefin blends. It can be noticed that carbonyl index of MPWS is significantly higher (almost 2 times) than that of prime blend, both before exposure and after 4 weeks of exposure. This observation suggests that MPWS are more susceptible to photodegradation as compared to the prime blend. In other words, polyolefin waste may require more additive to prevent photodegradation.
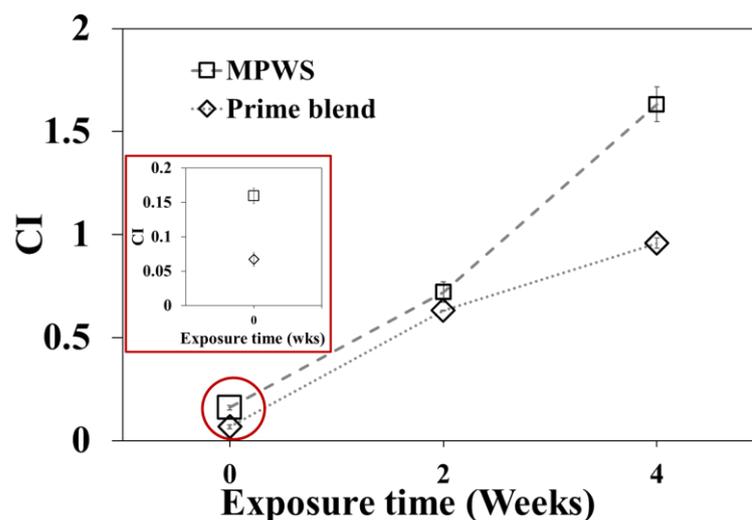

Figure 4. CI of prime polyolefin blend and MPWS as function of exposure time. Dotted lines are used to guide reader's eyes.

Figure 5a,b represent the CI of FLG-filled MPWS and prime polyolefin composites as a function of UV exposure time. It can be seen that the carbonyl formation rate in unfilled polyolefin blend (both waste and control) is much higher than FLG-filled composites. In the case of MPWS composites containing higher concentration of FLG (>1 wt.%), CI starts to increase only after 2 weeks of exposure. A higher value of CI is observed after 4 weeks of exposure in the MPWS composites, irrespective of the concentration of FLG. Interestingly, a decelerated growth of CI in MPWS composites is observed with higher concentrations of FLG. In contrast, based on CI value, carbonyl formation is not evident in FLG-filled prime blend composites over the entire UV exposure period. This holds true for both 0.5 and 1 wt.% FLG dosage in the control blend. Eventual retardation and termination of carbonyl formation in UV-exposed MPWS and prime polyolefin blend composites, respectively, indicate the photostabilizing potential of FLG. Moreover, this finding also suggests that the addition and mixing of a small amount of FLG in polyolefins prior to real-life applications would extend the lifespan of commodities made of polyolefins. It is worth mentioning that in an earlier publication by the co-authors [8], an Electron Paramagnetic Resonance (EPR) analysis was conducted to investigate the performance of FLG as a photostabilizer. The study reported that FLG effectively attenuates the characteristic EPR signal intensity, indicating both UV absorption/reflection and the scavenging of free radicals by FLG.
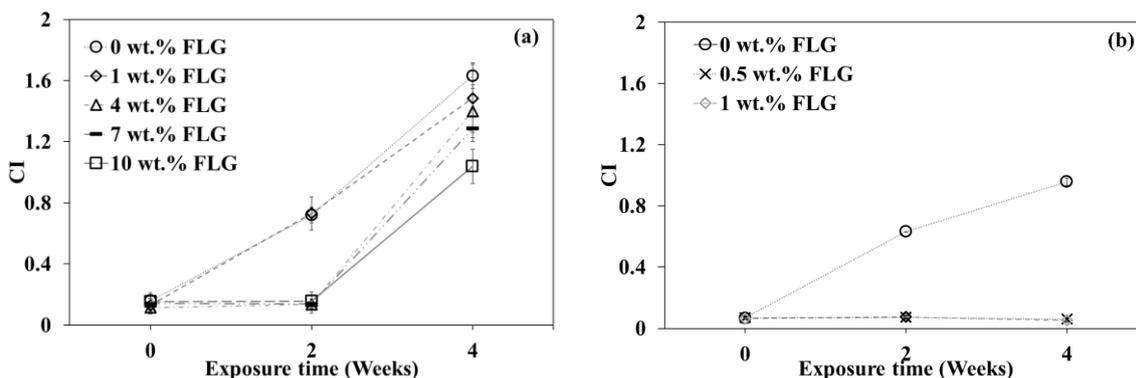
Figure 5. CI of (**a**) MPWS/FLG and (**b**) FLG-filled prime polyolefin composite as a function of UV exposure time. Dotted lines are used to guide reader's eyes.

2.3.2. Surface Appearance

Figure 6a,b show the surface finish of unfilled MPWS and 1 wt.% FLG-filled MPWS composite, after 4 weeks of exposure to UV radiation. In addition, Figure 6c,d showcase the surface finish of both the neat PE/PP blend and the PE/PP blend composites with 0.5 wt.% FLG, after a 4 week exposure to UV light. As a result of photodegradation, numerous longitudinal and transverse cracks appeared on the surface of neat MPWS sample. Although several cracks are observed after UV exposure on the MPWS/FLG composite with 1 wt.% FLG, the quantity is considerably reduced when compared to that of unfilled-MPWS. Similar to the case of MPWS, many longitudinal and transverse cracks are evident on the unfilled and UV exposed prime PE/PP blend surface. However, in contrast to the FLG-filled MPWS composite, there are no visible cracks on the surface of FLG-filled prime PE/PP blend composite. These observations suggest that even an FLG concentration as low as 0.5 wt.% is adequate to provide satisfactory UV protection to prime PE/PP, although not to mixed polyolefins waste-based compounds. The likely reasons for this are discussed in the subsequent section of this work.
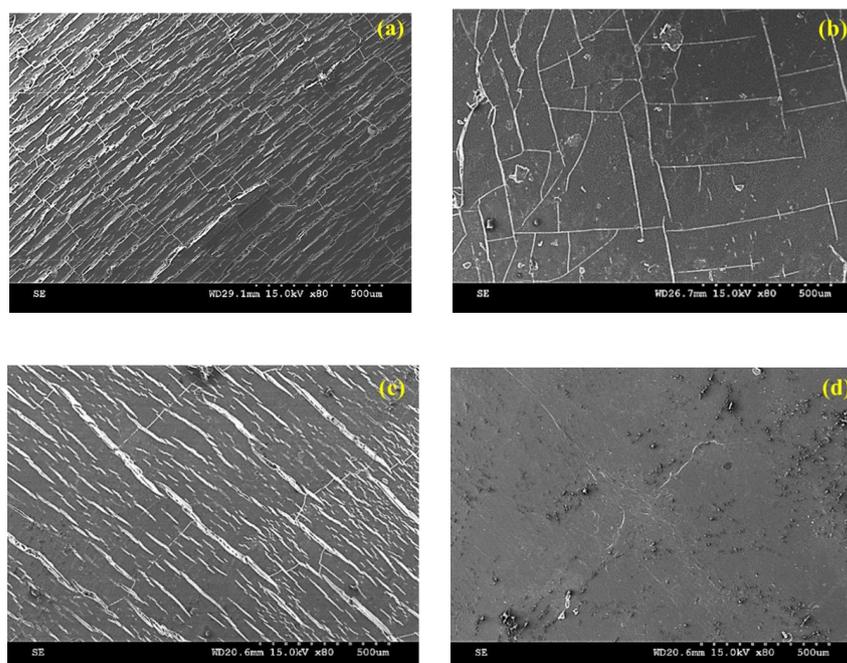

Figure 6. SEM images of the surfaces of (**a**) MPWS without FLG, (**b**) MPWS with 1 wt.% FLG, (**c**) Prime blend without FLG, and (**d**) Prime blend with 1 wt.% FLG; after 4 weeks of UV exposure.

To have an overview of crack formation, the crack density on the surface of UV-exposed samples has been calculated. Figure 7 shows crack density of FLG-filled MPWS and prime blend composites, after 4 weeks of UV exposure, as a function of FLG concentration. Photodegradation-driven crack density on the surface of UV-exposed MPWS compounds decreases as the concentration of FLG is increased in the composite. A concentration of FLG > 4 wt.% can effectively prevent crack formation (SEM images of the corresponding samples, Figure S1a,b, are provided in the Supplementary Information Section). On the other hand, 1 wt.% FLG is considered sufficient to prevent crack formation on the composite surface during UV exposure. These observations indicate that the presence of FLG slows down the UV degradation of polyolefin blends.
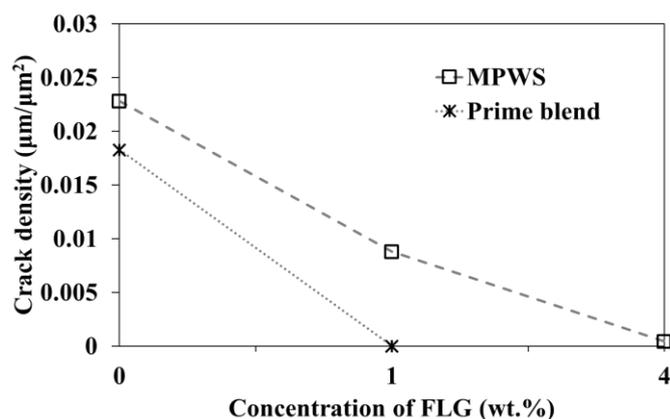

Figure 7. Crack density of MPWS/FLG composites, after 4 weeks of UV exposure, as a function of concentration of FLG.

2.3.3. Mechanical Properties

Figure 8a,b present the elongation at break and the impact strength of FLG-filled MPWS composites, respectively, plotted along primary Y-axis as a function of the concentration of FLG. The retention of the respective properties after 4 weeks of UV exposure is plotted along the secondary Y-axis. it is worth mentioning that the error bars (indicating standard deviation) for the ductility of unprocessed and unfilled MPWS are considerably wider compared to the performance of any of the other composites depicted in the Figure 8a. Experimental results suggest that the mixed polyolefin waste stream possesses a higher polydispersity or inhomogeneity. Conversely, the error bars associated with the ductility of the FLG-filled composites exhibit relatively smaller variations. This can be ascribed to the homogenizing influence of FLG, a phenomenon previously noted by the coauthors in a blend of recycled and prime PE in a prior study [42]. In addition, Figure 8c,d represent the retention of elongation at break and impact strength, respectively, of prime PE/PP blend composites after 4 weeks of UV exposure as a function of the concentration of FLG. In these figures, the unfilled bars correspond to the performance of neat (unfilled) blend, while black bars represent the composites where FLG was premixed with PE, and grey bars stand for the samples where FLG was premixed with PP.

As noticed in Figure 8a, the presence of FLG resulted in a reduction in the ductility of the MPWS composites compared to that of neat MPWS, as reported previously [3]. Notably, a 65% reduction in ductility is observed with the addition of 1 wt.% FLG. Further additions of 4, 7, and 10 wt.% FLG resulted in 68%, 77% and 80% reduction in original ductility, respectively. This reduction in the ductility of polymer blend composite is attributed to the compromised mobility of polymer chains, due to the presence of rigid fillers. A similar observation was reported earlier by other authors [46–48]. In contrast, an increment in the ductility of rigid filler-filled polymer blend composite, facilitated by the positive effect of good dispersion of filler and a strong matrix/filler interaction, was also reported in the literature [49,50]. After 4 weeks of UV exposure, around 20% of the original ductility is preserved in neat MPWS. Contrary to neat MPWS, around 60% of the original ductility

is preserved in MPWS composites containing 1 and 4 wt.% FLG. Remarkably, an even higher (~90%) ductility retention is observed in MPWS composites, containing 10 wt.% FLG. This finding suggests that the presence of FLG slows down the photodegradation of mixed polyolefin waste stream. A similar photostabilization effect of this commercially available FLG has also been reported in high-density polyethylene by the co-authors of this work [8]. In line with the observation from Figure 8a, it is evident in Figure 8b that the impact strength retention of UV-exposed MPWS is significantly lower compared to that of FLG-filled MPWS composites. Conversely, the tensile modulus and tensile strength retention for each of the exposed samples are well above 90% (see Figure S2a,b in the Supplementary Information Section), indicating that these properties of the polymeric materials have been less sensitive to UV exposure, at least for the irradiation duration adopted in this study. Similar observations were reported by other authors in unfilled-polyolefin blends [41]. Polymers undergo simultaneous chain scission and crosslinking during photo degradation [8,51]. Chain scission (negative effect) and crosslinking (positive effect) have two opposing effects on both the strength and stiffness of polymeric material. Therefore, changes in tensile strength and modulus are not clearly evident in the initial stage of UV exposure. However, after a certain period of irradiation, the negative effect of chain scission on tensile strength and modulus becomes predominant, resulting in reductions in the respective properties.
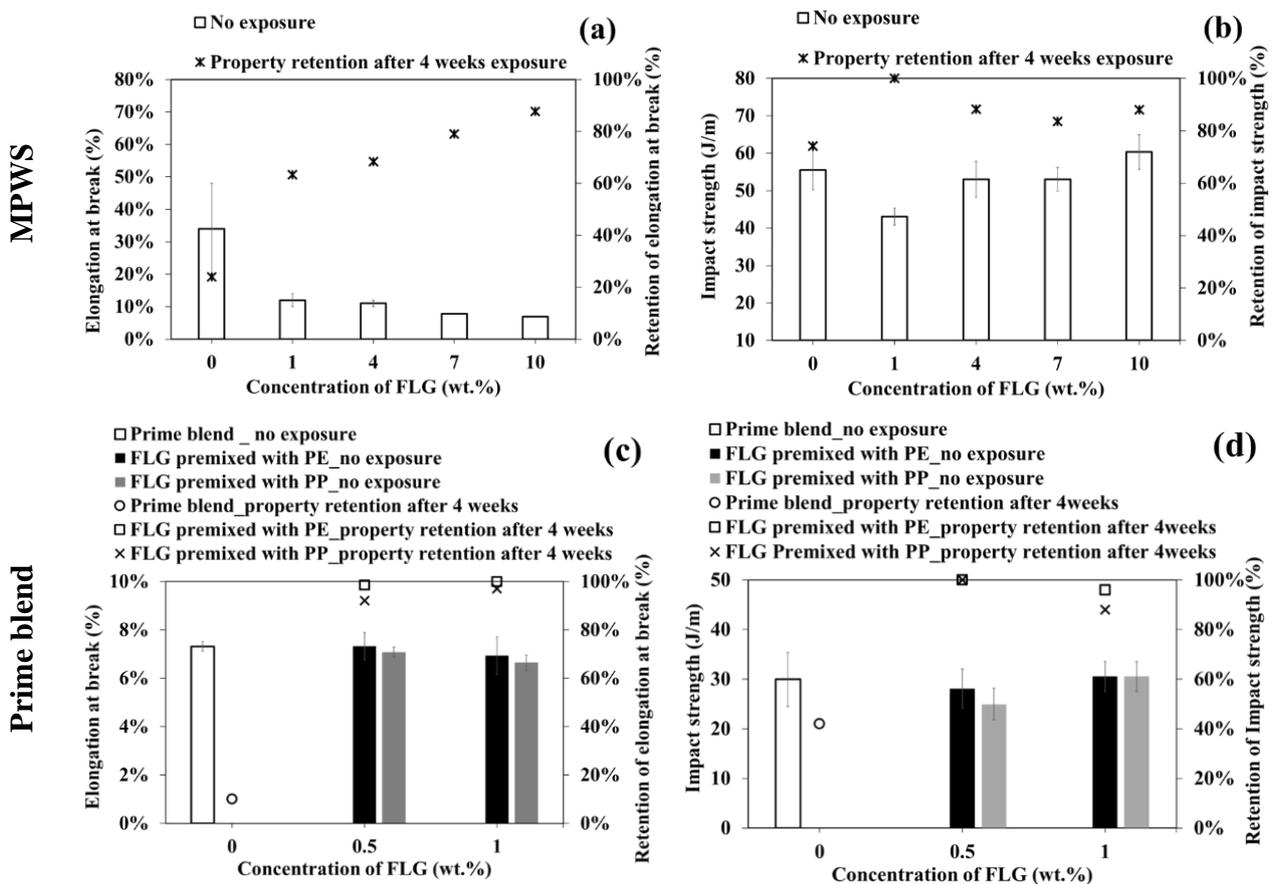

Figure 8. (**a**) Elongation at break along with retention of elongation at break (after UV exposure); (**b**) impact strength along with retention of impact strength (after UV exposure) of MPWS/FLG composites as a function of FLG concentration; (**c**) elongation at break along with retention of elongation at break (after UV exposure); (**d**) impact strength along with retention of impact strength (after UV exposure) of prime PE/PP blend composites as a function of FLG concentration, present in the composites.

Similar to aforementioned observations, Figure 8c,d show that the property retention of neat-prime PE/PP after 4 weeks of UV exposure is much less than those of FLG-filled prime PE/PP blend composites. However, a higher property retention is noted in FLG-filled prime blend composites after UV exposure, irrespective of the FLG mixing strategy. In contrast to the case of MPWS/FLG composites, a higher percentage of ductility and impact toughness is preserved in UV-exposed prime PE/PP composite at a very low concentration of FLG (0.5 or 1 wt.%). This can be explained by the poor dispersion of FLG in MPWS compared to that of prime polyolefin blend, as presented in Figure 3a–c. The associated findings reinforce the notion that the same FLG concentration has a more pronounced influence on the prime polyolefin blend compared to MPWS. Moreover, the presence of higher carbonyl content in the MPWS (being a mix of recycled polymers) than in the prime blend (shown in Figure 4) indicates that a higher dosage of FLG would be required to slow down the photodegradation process of pre-degraded polyolefin waste like the MPWS used in this work.

2.4. Discussions

The results show that the addition of FLG is an efficient strategy to slow down the photodegradation processes in polyolefin blends, both recovered post-consumer waste mixture and prime polyolefin blends. Photodegradation of the samples has been investigated in terms of the carbonyl concentration increase, crack density and mechanical property retention of the compounds after 4 weeks of UV exposure. Table 2 highlights the photoprotection effect of FLG in a waste and prime polyolefin mixture.

Table 2. Change in carbonyl index (CI), crack density and retention of ductility after 4 weeks of UV exposure in MPWS and prime blend composites as a function of concentration of FLG.

Parameters	MPWS					Prime Blend (FLG Premixed with PE)		
Concentration of FLG (wt.%)	0	1	4	7	10	0	0.5	1
Change in CI (%)	1069	964	903	821	645	1325	No significant change	
Crack density ($\mu m/\mu m^2$)	0.0228	0.0088	0.0004	No visible cracks but surface delamination		0.0182		
Retention of ductility (%)	20	60	70	80	90	10		

Based on the information presented in Table 2, the efficiency of FLG as a photostabilizer is more evident in prime polyolefin blend than in mixed plastic waste. The findings of Figure 3c help to explain this observation. The plot outlines that FLG was poorly dispersed in MPWS compared to prime PE/PP blend composites, prepared under the same processing conditions. It has been reported in the literature [8] that FLG mostly slows down the photodegradation of polymer material via UV absorption/reflection and free radical scavenging. Moreover, FLG also acts as a physical barrier to oxygen which limits the oxygen penetration through the polymer, which also minimizes the photooxidative degradation of the respective plastic material. Therefore, poor dispersion of FLG in polymeric material leads to less efficient utilization of FLG.

Additionally, polyolefins are ideally expected to be resistant to photodegradation as they do not have any unsaturated chromophores or carbon bonds in their backbone. However, external impurities or structural defects can initiate the photodegradation process, resulting in chain scission and eventual formation and accumulation of carbonyl groups. These initial unsaturated double bonds of carbonyl groups cause polyolefins to be more susceptible to photodegradation. Therefore, comparatively less photoprotection attained in FLG-filled waste polyolefins mixture than that of controlled composites could be attributed to the inherent uncertainties associated with plastic waste, such as the presence of impurities, presence of pre-degraded polymer chains, and polydispersity. Larger standard deviations of ductility and comparatively higher carbonyl index of waste

polyolefin mixture (compared to prime polyolefin blend of this work) present experimental evidence that supports the fact that more inhomogeneity and predegraded plastic are present in MPWS. Hence, the combination of a comparatively poor dispersion of FLG with the presence of impurities and predegraded elements in MPWS makes this mixture more susceptible to photodegradation, requiring more dosage of FLG to attain a satisfactory level of photoprotection.

In this context, it is noteworthy to highlight the findings of Figure 5b. The plot indicates no carbonyl growth in UV-exposed primary polyolefin composites after a 4-week UV exposure period. In other words, the photodegradation of prime polyolefin was significantly decelerated due to the presence of FLG. This insight implies the recommendation of adding FLG into polyolefins as a pretreatment step. It is expected that post-consumer polyolefin waste generated from FLG-filled polyolefin will experience reduced photodegradation, resulting in both an extended lifespan and requiring a smaller quantity of FLG for the photoprotection of the subsequent MPWS for reuse.

Concurrently, this study has investigated the impact of selectively localized FLG in different phases of the blend on the retardation of photodegradation. By employing a premixing approach, FLG was predominantly located within either the PP or PE phase of the prime polyolefin blend. The results indicate that the efficiency of FLG as a photostabilizer remains unaffected by its preference to a specific phase. This could be attributed to the inherent qualities of FLG as a photostabilizer, which are not significantly influenced by or contingent upon its selective localization in the blend. It is worth noting that this finding underscores the application of FLG as a suitable photostabilizing additive for MPWS, especially in scenarios where achieving predominant selective localization of unfunctionalized FLG is unattainable.

3. Materials and Methods

3.1. Materials

FLG powder (GrapheneBlack 3X) from NanoXplore Inc., Montreal, QC, Canada, was used in this work. This grade of FLG typically consists of 6 to 10 atomic layers. The primary particles exhibit a lateral size ranging from 1 to 2 μm. These primary particles, in a dry powder state, form loose clusters also known as secondary particles. The average lateral size of these secondary particles is approximately 30 μm.

For this study, a mixed polyolefins waste mixture was obtained from a local recycler in Quebec. The information provided by the supplier indicates that the mixture comprises polyethylene (PE) along with approximately 30 to 40 wt.% polypropylene (PP) and ≤5 wt.% contamination (such as dye, ink, or pigment). Differential scanning calorimetry (DSC) analyses were used to assess the composition of the mixture (PE/PP—60/40), as reported in our previous work [3].

A prime PE/PP—60/40 blend was prepared, replicating the morphology of MPWS blends. To maintain controlled and simplified conditions, the prime blend was investigated both without FLG and with FLG, excluding other impurities or uncertainties likely associated with MPWS. Table 3 outlines the identification and MFI of the polymers used in this work.

Table 3. Identification and MFI of the polymers used in this work.

Polymer	Commercial Name	MFI (g/10 min)
MPWS	N/A	≥4 (230 °C, 2.16 kg)
PE	Formolene HB5502B	0.35 (190 °C/2.16 kg)
PP	Polypropylene 3720 WZ	20 (230 °C, 2.16 kg)

3.2. Methods

In this study, master batch (MB) pellets composed of FLG and polymers (PE, PP, or MPWS) were utilized to prepare the composites.

In the case of MPWS/FLG composites, the MPWS/FLG MB was further diluted with MPWS to prepare composites with 1, 4, 7 and, 10 wt.%. of FLG, respectively.

In addition, FLG-filled prime PE/PP blend composites were prepared through a two-step process. In the initial step, PE/FLG or PP/FLG MB was diluted with PE or PP, respectively, which can be referred as a premixing step. In the subsequent step, these pre-mixed composites were melt-blended with the other corresponding polymer of the PE/PP blend. Prime PE/PP blend composites containing 0.5 and 1 wt.% FLG were also prepared in this work, via FLG pre-mixing with PE or PP. All the samples were processed in a HAAKE twin-screw extruder, (Rheomex OS PTW16/40, manufactured by Thermo Fisher Scientific, Dreieich, Germany) at 150 rpm, and 200 °C in all zones.

Extruded pellets were injection molded to prepare specimens for tensile and impact property analysis. Injection molding was performed using the Arburg Allrounder 221K-350-100 Injection molding machine (manufactured by Arburg GmbH + Co. KG, Loßburg, Germany).

3.3. Photodegradation Process

The injected specimens were subjected to an accelerated weathering condition by using a QUV chamber, equipped with UVA-340 type lamps. According to the guidelines of cycle A outlined in ASTM G154 [52] the samples were exposed to an irradiation of 0.89 W/m^2 at 60 °C for 8 h, followed by 4 h of water condensation at 50 °C. The specimens were taken out of the QUV chamber after exposure durations of 2 weeks (336 h) and 4 weeks (672 h).

3.4. Characterizations

Scanning Electron Microscope (SEM) images of the UV-exposed surfaces of the samples were obtained using a Hitachi SEM S3600-N (Model: MEB-3600-N, manufactured by Hitachi Science Systems, Ltd., Tokyo, Japan). Before imaging, the surface of the compounds was coated with a thin layer of gold using a Gold Sputter Coater (Model: K550X, manufactured by Quorum Technologies Ltd., East Sussex, UK). This gold coating enhances the conductivity of the samples and provides better imaging results in the SEM. To investigate the microstructure, the compression molded samples were cryo-fractured, prior to gold coating.

The optical microscope images of compression molded thin films of 1 wt.% FLG-filled MPWS and prime PE/PP blend composites were observed using an optical microscope (Model: Olympus BX51, manufactured by Olympus Corporation, Tokyo, Japan) in transmission mode. A minimum of 10 images were taken from different areas of the films. Subsequently, ImageJ software (version number: 1.52a) was utilized to evaluate the FLG dispersion within the various matrices. Before the quantitative assessment of filler dispersion, image preprocessing steps involving noise reduction and removal of the polymeric matrix background were executed by using the ImageJ software. Moreover, length of the surface crack of UV-exposed samples was determined by using ImageJ software to determine crack density using the following Equation (1):

$$\text{Crackdensity} = \frac{\sum Crack\ length\ (\mu m)}{Area\ under\ consideration\ (\mu m^2)} \tag{1}$$

Melt flow index (MFI) of mixed polyolefin waste and prime polyolefin blend was investigated using an MFI tester (manufactured by International Equipments, Mumbai, India). ASTM D1238 [53] was followed to measure MFI.

ATR-FTIR spectra of the thin films of neat and FLG-filled composites were captured using a FTIR spectrometer (manufactured by PerkinElmer, Llantrisant, UK) the Spectrum Two™, equipped with a diamond crystal. A number of 10 scans were acquired with a resolution of $4\,\text{cm}^{-1}$ within the wave numbers range of 400–$4000\,\text{cm}^{-1}$. These spectra were used to assess the carbonyl index (CI) of each of the samples, with the following Equation (2):

$$\text{CI} = \frac{A_{C=O}}{A_{CH_2}} \tag{2}$$

Here, $A_{C=O}$ is the peak area within 1680–1800 cm^{-1} wave number range and A_{CH_2} is the peak areas within 680–760 cm^{-1} wave number range, representing C=O and CH$_2$ functional groups, respectively. The assessment of CI is interesting because it is an indicator of the degradation of polymer during its lifespan. At least three spectra from different parts of each sample were considered to calculate and report the average CI values with standard deviation as error bars.

The tensile properties of the samples were investigated using an MTS Alliance RF/200 tensile test apparatus (manufactured by MTS Systems Corporation, Eden Prairie, MN, USA), following the guidelines outlined in the ASTM D638 [54]. The tests were conducted at room temperature with a 10 kN load, and a crosshead speed of 50 mm/min. The key parameters analyzed include tensile strength, tensile modulus, and elongation at break.

The notched impact strength of the samples was determined using an impact strength tester device (manufactured by International Equipments, India). The measurement was carried out in accordance with the ASTM D256 [55]. To create notches in the samples, a motorized notch cutter (manufactured by International Equipments, India) was utilized. For each composite, at least five specimens were tested to investigate tensile and impact properties. In the subsequent sections of this report, we have graphically depicted the property (elongation at break, impact strength, tensile strength, and modulus) retention (%) of the composites after UV exposure as a function of FLG concentration within the composite. The graphical representation of property retention (%) has been adopted to portray the precise influence of adding FLG on the retardation of photodegradation of polyolefin blend. Property retention (%) has been calculated according to the following Equation (3):

$$\text{Property retention}(\%) = \frac{\text{Property after UV}}{\text{Property before UV}} \times 100\% \qquad (3)$$

4. Conclusions

This work presents that FLG can successfully slow down the photodegradation processes in polyolefins blends. This observation is valid for both a plastic waste recovered polyolefins blend and a control prime polyolefin blend, ensuring longer lifespan of polyolefins blends used for outdoor applications. The main findings of this work can be concluded with the following points:

- The addition of FLG can effectively slow down the photodegradation of polyolefins blends.
- Although FLG exhibits a thermodynamic preference for PE over PP, the photostabilization of a PE/PP blend is not significantly affected by the selective distribution of FLG in either phase.
- A mere 0.5 wt.% or 1 wt.% of FLG is found sufficient to ensure the photostability of a prime PE/PP blend.
- To ensure better photoprotection in recycled polymer blends, a higher concentration of FLG is required, attributed partly to the predegraded condition of MPWS.
- Furthermore, pretreatment of prime polyolefins with FLG could be a recommended step, which, in turn, would extend the lifespan and generate a less degraded MPWS for potential reuse.

This work underscores the potential to extend the lifespan of polyolefins, thereby decreasing the generation of plastic waste, through the addition of commercially available and low-cost FLG, produced in compliance with Canadian environmental regulations. By extending the use of plastic products, their entry into waste streams is delayed. Moreover, extending the lifespan of products is anticipated to decrease the demand for new ones. Thus, this study presents a promising method to elevate the value of MPWS, intrinsically with minimum worth, that would otherwise be relegated to landfill disposal.

Data Availability Statement: The data presented in this study can be found within the article and its Supplementary Material Section. Raw data that supports the findings of this work can be inquired to the corresponding authors, upon reasonable request.

Conflicts of Interest: The authors declare no conflicts of interest.

References

1. Singh, M.K.; Mohanty, A.K.; Misra, M. Upcycling of waste polyolefins in natural fiber and sustainable filler-based biocomposites: A study on recent developments and future perspectives. *Compos. Part B Eng.* **2023**, *263*, 110852. [CrossRef]
2. Jubinville, D.; Esmizadeh, E.; Saikrishnan, S.; Tzoganakis, C.; Mekonnen, T. A comprehensive review of global production and recycling methods of polyolefin (PO) based products and their post-recycling applications. *Sustain. Mater. Technol.* **2020**, *25*, e00188. [CrossRef]
3. Sultana, S.M.N.; Helal, E.; Guti, G.; David, E.; Moghimian, N.; Demarquette, N.R. Effect of Few-Layer Graphene on the Properties of Mixed Polyolefin Waste Stream. *Crystals* **2023**, *13*, 358. [CrossRef]
4. Fang, C.; Nie, L.; Liu, S.; Yu, R.; An, N.; Li, S. Characterization of polypropylene-polyethylene blends made of waste materials with compatibilizer and nano-filler. *Compos. Part B Eng.* **2013**, *55*, 498–505. [CrossRef]
5. Karaagac, E.; Koch, T.; Archodoulaki, V.M. The effect of PP contamination in recycled high-density polyethylene (rPE-HD) from post-consumer bottle waste and their compatibilization with olefin block copolymer (OBC). *Waste Manag.* **2021**, *119*, 285–294. [CrossRef] [PubMed]
6. Najafi, S.K.; Hamidinia, E.; Tajvidi, M. Mechanical properties of composites from sawdust and recycled plastics. *J. Appl. Polym. Sci.* **2006**, *100*, 3641–3645. [CrossRef]
7. Kazemi, Y.; Kakroodi, A.R.; Rodrigue, D. Compatibilization Efficiency in Post-Consumer Recycled Polyethylene/Polypropylene Blends: Effect of Contamination. *Polym. Eng. Sci.* **2015**, *55*, 2368–2376. [CrossRef]
8. Karimi, S.; Helal, E.; Gutierrez, G.; David, E.; Samara, M.; Demarquette, N. Photo-stabilization mechanisms of High-Density Polyethylene (HDPE) by a commercial few-layer graphene. *Polym. Eng. Sci.* **2023**, *63*, 3879–3890. [CrossRef]
9. Gutiérrez-Villarreal, M.H.; Zavala-Betancourt, S.A. A Comparative Study of the Photodegradation of Two Series of Cyclic Olefin Copolymers. *Int. J. Polym. Sci.* **2017**, *2017*, 1870814. [CrossRef]
10. Ojeda, T.; Freitas, A.; Birck, K.; Dalmolin, E.; Jacques, R.; Bento, F.; Camargo, F. Degradability of linear polyolefins under natural weathering. *Polym. Degrad. Stab.* **2011**, *96*, 703–707. [CrossRef]
11. Peng, Y.; Guo, X.; Cao, J.; Wang, W. Effects of two staining methods on color stability of wood flour/polypropylene composites during accelerated UV weathering. *Polym. Compos.* **2017**, *38*, 1194–1205. [CrossRef]
12. Yousif, E.; Haddad, R. Photodegradation and Photostabilization of Polymers, Especially Polystyrene: Review. *SpringerPlus* **2013**, *2*, 398. [CrossRef] [PubMed]
13. Rabek, J.F. *Polymer Photodegradation: Mechanisms and Experimental Methods*; Chapman & Hall: London, UK, 1995.
14. Rånby, B. Photodegradation and photo-oxidation of synthetic polymers. *J. Anal. Appl. Pyrolysis* **1989**, *15*, 237–247. [CrossRef]
15. Karimi, S.; Helal, E.; Gutierrez, G.; Moghimian, N.; Madinehei, M.; David, E.; Samara, M.; Demarquette, N. A Review on Graphene's Light Stabilizing Effects for Reduced Photodegradation of Polymers. *Crystals* **2021**, *11*, 3. [CrossRef]
16. Waldman, W.R.; De Paoli, M.A. Photodegradation of polypropylene/polystyrene blends: Styrene-butadiene-styrene compatibilisation effect. *Polym. Degrad. Stab.* **2008**, *93*, 273–280. [CrossRef]
17. Kumar, A.P.; Depan, D.; Tomer, N.S.; Singh, R.P. Nanoscale particles for polymer degradation and stabilization-Trends and future perspectives. *Prog. Polym. Sci.* **2009**, *34*, 479–515. [CrossRef]

18. Gijsman, P.; Jan, H.; Daan, T. The mechanism of action of hindered amine light stabilizers. *Polym. Degrad. Stab.* **1993**, *39*, 225–233. [CrossRef]

19. Chaudhuri, I.; Fruijtier-Pölloth, C.; Ngiewih, Y.; Levy, L. Evaluating the evidence on genotoxicity and reproductive toxicity of carbon black: A critical review. *Crit. Rev. Toxicol.* **2018**, *48*, 143–169. [CrossRef]

20. Tipton, D.A.; Lewis, J.W. Effects of a hindered amine light stabilizer and a UV light absorber used in maxillofacial elastomers on human gingival epithelial cells and fibroblasts. *J. Prosthet. Dent.* **2008**, *100*, 220–231. [CrossRef]

21. Alotaibi, M.D.; McKinley, A.J.; Patterson, B.M.; Reeder, A.Y. Benzotriazoles in the Aquatic Environment: A Review of Their Occurrence, Toxicity. *Degrad. Anal. Water Air Soil Pollut.* **2015**, *226*, 226. [CrossRef]

22. Johra, F.T.; Lee, J.W.; Jung, W.G. Facile and safe graphene preparation on solution based platform. *J. Ind. Eng. Chem.* **2014**, *20*, 2883–2887. [CrossRef]

23. Dash, G.N.; Pattanaik, S.R.; Behera, S. Graphene for electron devices: The panorama of a decade. *IEEE J. Electron Devices Soc.* **2014**, *2*, 77–104. [CrossRef]

24. Yoo, B.M.; Shin, H.J.; Yoon, H.W.; Park, H.B. Graphene and graphene oxide and their uses in barrier polymers. *J. Appl. Polym. Sci.* **2014**, *131*, 39628. [CrossRef]

25. Cui, Y.; Kundalwal, S.I.; Kumar, S. Gas barrier performance of graphene/polymer nanocomposites. *Carbon* **2016**, *98*, 313–333. [CrossRef]

26. Junior, J.C.F.; Moghimian, N.; Gutiérrez, G.; Helal, E.; Ajji, A.; de Oliveira Barra, G.M.; Demarquette, N.R. Effects of an industrial graphene grade and surface finishing on water and oxygen permeability, electrical conductivity, and mechanical properties of high-density polyethylene (HDPE) multilayered cast films. *Mater. Today Commun.* **2022**, *31*, 103470. [CrossRef]

27. Moghimian, N.; Nazarpour, S. The future of carbon: An update on graphene's dermal, inhalation, and gene toxicity. *Crystals* **2020**, *10*, 718. [CrossRef]

28. de Oliveira, Y.D.C.; Amurin, L.G.; Valim, F.C.F.; Fechine, G.J.M.; Andrade, R.J.E. The role of physical structure and morphology on the photodegradation behaviour of polypropylene-graphene oxide nanocomposites. *Polymer* **2019**, *176*, 146–158. [CrossRef]

29. Mistretta, M.C.; Botta, L.; Vinci, A.D.; Ceraulo, M.; La Mantia, F.P. Photo-oxidation of polypropylene/graphene nanoplatelets composites. *Polym. Degrad. Stab.* **2019**, *160*, 35–43. [CrossRef]

30. Moon, Y.; Yun, J.; Kim, H.; Lee, Y. Effect of graphite oxide on photodegradation behavior of poly (vinyl alcohol)/graphite oxide composite hydrogels. *Carbon Lett.* **2011**, *12*, 138–142. [CrossRef]

31. Hasani, M.; Mahdavian, M.; Yari, H.; Ramezanzadeh, B. Versatile protection of exterior coatings by the aid of graphene oxide nano-sheets; comparison with conventional UV absorbers. *Prog. Org. Coat.* **2018**, *116*, 90–101. [CrossRef]

32. Goodwin, D.G.; Shen, S.J.; Lyu, Y.; Lankone, R.; Barrios, A.C.; Kabir, S.; Perreault, F.; Wohlleben, W.; Nguyen, T.; Sung, L. Graphene/polymer nanocomposite degradation by ultraviolet light: The effects of graphene nanofillers and their potential for release. *Polym. Degrad. Stab.* **2020**, *182*, 109365. [CrossRef] [PubMed]

33. Nuraje, N.; Khan, S.I.; Misak, H.; Asmatulu, R. The Addition of Graphene to Polymer Coatings for Improved Weathering. *ISRN Polym. Sci.* **2013**, *2013*, 514617. [CrossRef]

34. La Mantia, F.P.; Morreale, M.; Botta, L.; Mistretta, M.C.; Ceraulo, M.; Scaffaro, R. Degradation of polymer blends: A brief review. *Polym. Degrad. Stab.* **2017**, *145*, 79–92. [CrossRef]

35. Christensen, P.A.; Egerton, T.A.; Martins-Franchetti, S.M.; Jin, C.; White, J.R. Photodegradation of polycaprolactone/poly(vinyl chloride) blend. *Polym. Degrad. Stab.* **2008**, *93*, 305–309. [CrossRef]

36. Fernandes, L.; Freitas, C.A.; Demarquette, N.R.; Fechine, G.J.M. Photodegradation of Thermodegraded Polypropylene/ High-Impact Polystyrene Blends: Mechanical Properties. *J. Appl. Polym. Sci.* **2010**, *120*, 770–779. [CrossRef]

37. Halina, K. Photodegradation of Polystyrene and Poly(vinyl acetate) Blends-I. Irradiation of PS/PVAc blends by Polychromatic Light. *Eur. Polym. J.* **1995**, *31*, 1037–1042.

38. Mailhot, B.; Morlat, S.; Gardette, J.L. Photooxidation of blends of polystyrene and poly(vinyl methyl ether): FTIR and AFM studies. *Polymer* **2000**, *41*, 1981–1988. [CrossRef]

39. Rivaton, A.; Serre, F.; Gardette, J.L. Oxidative and photooxidative degradations of PP/PBT blends. *Polym. Degrad. Stab.* **1998**, *62*, 127–143. [CrossRef]

40. Ołdak, D.; Kaczmarek, H.; Buffeteau, T.; Sourisseau, C. Photo- and bio-degradation processes in polyethylene, cellulose and their blends studied by ATR-FTIR and raman spectroscopies. *J. Mater. Sci.* **2005**, *40*, 4189–4198. [CrossRef]

41. Al-Salem, S.M.; Al-Dousari, N.M.; Abraham, G.J.; D'souza, M.A.; Al-Qabandi, O.A.; Al-Zakri, W. Effect of Die Head Temperature at Compounding Stage on the Degradation of Linear Low Density Polyethylene/Plastic Film Waste Blends after Accelerated Weathering. *Int. J. Polym. Sci.* **2016**, *2016*, 8–11. [CrossRef]

42. López-Martínez, E.D.; Martínez-Colunga, J.G.; Ramírez-Vargas, E.; Sanchez-Valdes, S.; Ramos-de Valle, L.F.; Benavides-Cantu, R.; Rodríguez-Gonzalez, J.A.; Mata-Padilla, J.M.; Cruz-Delgado, V.J.; Borjas-Ramos, J.J.; et al. Influence of carbon structures on the properties and photodegradation of LDPE/LLDPE films. *Polym. Adv. Technol.* **2022**, *33*, 1727–1741. [CrossRef]

43. Diallo, A.K.; Helal, E.; Gutiérrez, G.; Madinehei, M.; David, E.; Demarquette, N.; Moghimian, N. Graphene: A multifunctional additive for sustainability. *Sustain. Mater. Technol.* **2022**, *33*, e00487. [CrossRef]

44. Tu, C.; Nagata, K.; Yan, S. Influence of melt-mixing processing sequence on electrical conductivity of polyethylene/polypropylene blends filled with graphene. *Polym. Bull.* **2017**, *74*, 1237–1252. [CrossRef]

45. Kasaliwal, G.R.; Göldel, A.; Pötschke, P.; Heinrich, G. Influences of polymer matrix melt viscosity and molecular weight on MWCNT agglomerate dispersion. *Polymer* **2011**, *52*, 1027–1036. [CrossRef]

46. Abbasi, F.; Shojaei, D.A.; Bellah, S.M. The compatibilization effect of exfoliated graphene on rheology, morphology, and mechanical and thermal properties of immiscible polypropylene/polystyrene (PP/PS) polymer blends. *J. Thermoplast. Compos. Mater.* **2019**, *32*, 1378–1392. [CrossRef]

47. Parameswaranpillai, J.; Joseph, G.; Shinu, K.P.; Jose, S.; Salim, N.V.; Hameed, N. Development of hybrid composites for automotive applications: Effect of addition of SEBS on the morphology, mechanical, viscoelastic, crystallization and thermal degradation properties of PP/PS-xGnP composites. *RSC Adv.* **2015**, *5*, 25634–25641. [CrossRef]

48. Haghnegahdar, M.; Naderi, G.; Ghoreishy, M.H.R. Electrical and thermal properties of a thermoplastic elastomer nanocomposite based on polypropylene/ethylene propylene diene monomer/graphene. *Soft Mater.* **2017**, *15*, 82–94. [CrossRef]

49. Pour, R.H.; Hassan, A.; Soheilmoghaddam, M.; Bidsorkhi, H.C. Mechanical, thermal, and morphological properties of graphene reinforced polycarbonate/acrylonitrile butadiene styrene nanocomposites. *Polym. Compos.* **2016**, *37*, 1633–1640. [CrossRef]

50. Bijarimi, M.; Amirul, M.; Norazmi, M.; Ramli, A.; Desa, M.S.Z.; Desa, M.A.; Samah, M.A.A. Preparation and characterization of poly (lactic acid) (PLA)/polyamide 6 (PA6)/graphene nanoplatelet (GNP) blends bio-based nanocomposites. *Mater. Res. Express* **2019**, *6*, 055044. [CrossRef]

51. Hocker, S.J.A.; Kim, W.T.; Schniepp, H.C.; Kranbuehl, D.E. Polymer crystallinity and the ductile to brittle transition. *Polymer* **2018**, *158*, 72–76. [CrossRef]

52. *ASTM G154*; Standard Practice for Operating Fluorescent Ultraviolet (UV) Lamp Apparatus for Exposure of Materials. ASTM International: West Conshohocken, PA, USA, 2023; p. 12.

53. *ASTM D1238*; Standard Test Method for Melt Flow Rates of Thermoplastics by Extrusion Plastometer. ASTM International: West Conshohocken, PA, USA, 2010; p. 15.

54. *ASTM D638*; Standard Test Method for Tensile Properties of Plastics. ASTM International: West Conshohocken, PA, USA, 2015; p. 17.

55. *ASTM D256*; Standard Test Methods for Determining the Izod Pendulum Impact Resistance of Plastics. ASTM International: West Conshohocken, PA, USA, 2023; p. 20.